Optimization of Magnetic Perturbation Spectra for the COMPASS Tokamak

P. Cahyna 1), R. Pánek 1), V. Fuchs 1), L. Krlín 1), M. Bécoulet 2), G. Huysmans 2), E. Nardon 3)

1) Institute of Plasma Physics AS CR v.v.i., Association EURATOM/IPP.CR, Prague, Czech Republic.
2) Association Euratom-CEA, IRFM, Cadarache, 13108, St-Paul-lez-Durance, France.
3) Euratom/UKAEA Fusion Association, Culham Science Centre, Abingdon, OX143DB, U.K.

e-mail contact of main author: cahyna@ipp.cas.cz

Abstract. The COMPASS tokamak, recently transferred from UKAEA Culham to IPP Prague, is equipped with a set of saddle coils for producing controlled resonant magnetic perturbations (RMPs). In the future experimental programme of COMPASS we plan to focus on studies of RMPs, especially in view of their application as an ELM control mechanism and their planned use in ITER. In the present contribution we describe the preparatory calculations for the planned experiments. We computed the spectra of perturbations for several different equilibra predicted by MHD simulations and determined the positions and sizes of the resulting islands. It is shown how the saddle coils of COMPASS can be adapted to our equilibria to obtain good island overlap at the edge, which is believed to be a key component in the ELM mitigation effect. Impact of the nonlinear plasma response on the perturbation field is discussed, using results of a cylindrical reduced MHD code.

1. Introduction

In past years there has been a growing interest in the physics of resonant magnetic perturbations (RMPs) applied externally to a tokamak plasma. The main motivation is that they are a promising tool to control Type I Edge Localized Modes (ELMs) – an important issue for ITER. The ability of mitigating ELMs has been discovered on DIII-D [1] and subsequently confirmed by recent experiments on JET [2]. Coils to induce RMPs for ELM mitigation will be present in the ITER design in some form. There are however still many open questions concerning the mechanism itself and related issues, and the theory of the mitigation effect is far from being complete.

The COMPASS tokamak, which is now being reinstalled in IPP Prague [3], is a device suitable for the research of magnetic perturbations. It is a tokamak with single-null divertor plasma and geometry similar to JET or ITER at a much smaller scale with the major radius of 0.56 m. Its unique feature is a rich set of "saddle coils" to produce magnetic perturbations. Our plan is to use them to investigate the effects associated with the ELM mitigation technique. Examples of effects which should be studied are: the pump-out effect associated with the impact on ELMs or the impact of perturbations on the plasma rotation by both resonant [4] and non-resonant braking [5], which is especially important for ITER. If we succeed in obtaining Type-I ELMs on the reinstalled COMPASS thanks to the new NBI heating system, it will be also possible to study the ELM mitigation effect directly.

In the present paper we present calculations of the perturbation field that we have done in preparation for the experiments with "saddle coils". We start with the analysis of spectra of the vacuum field. In this simplified model, the plasma response to the perturbation is not taken into account, the field is modelled as the plasma equilibrium field with the vacuum field from the saddle coils added. We use this approach to determine the optimal coil configuration for

producing sufficient island overlap at the edge, which is supposed to be the key effect for ELM mitigation. Knowledge of the required configuration will be important for adjusting the coils before the COMPASS operation starts.

As the procedure outlined above does not take into account modification of the perturbation field by the plasma response, we are currently performing reduced MHD simulations to evaluate this effect. The simulations are done with a code using simplified cylindrical geometry, taking into account the toroidal plasma rotation which is expected to reduce island sizes by screening the perturbation.

2.   Vacuum field calculations with the code ERGOS

Nonaxisymmetric perturbations of the tokamak magnetic field are able to produce magnetic islands. One mechanism through which the perturbation field may influence the plasma is the destruction of magnetic surfaces and stochastization of the field lines. This effect is linked to the magnetic islands, because it arises when neighboring island chains become large enough to overlap each other. The overlapping of magnetic islands at the plasma edge was proposed as the criterion for the ELM suppression effect, according to the observed correlations [6, 7]. We are therefore using the same criterion for evaluating the suitability of COMPASS for the research of the ELM suppression effect and for choosing among the configuration of the perturbation coils the one which will be optimal for this research.

In accordance with many previous works [6–9] we use the vacuum field of the perturbation coils superposed with the equilibrium field of the plasma in absence of the perturbation. This simple approach will be referred to as the "vacuum approximation". It neglects possible modification of the perturbation field by the presence of the plasma. We use this approach because of its proven ability to characterize the ELM suppression effect [6, 7], but we are aware that it might not be an accurate model of the actual magnetic field in the plasma.

The width of the magnetic islands is calculated according to the procedure described in [8, 10] in a magnetic coordinate system (s, θ^*, φ) where s is a dimensionless flux surface label defined as the square root of the normalized poloidal flux ψ: $s = \sqrt{\psi}$. The poloidal and toroidal angular coordinates θ^* and φ represent a field line as a line of a constant slope: $d\theta^*/d\varphi = 1/q(s)$ along a field line, where $q(s)$ is the safety factor on a surface given by s. In addition the coordinate φ is taken equal to the geometric toroidal angle. The magnetic islands are produced by the contravariant radial component of the perturbation field $B^1 = \delta\vec{B} \cdot \nabla s$, $\delta\vec{B}$ being the perturbation field. Islands appear at the rational values of the safety factor q and their size is determined by the Fourier component $\tilde{b}^1_{(m,n)}$ of B^1 normalized to the toroidal contravariant component B^3 of the equilibrium field: $B^3 = \vec{B} \cdot \nabla\varphi$. $\tilde{b}^1_{(m,n)}$ is thus defined by the equation

$$b^1 \equiv B^1/B^3 = \sum_{m,n} \tilde{b}^1_{(m,n)} \exp\left[i(m\theta^* - n\varphi)\right]. \tag{1}$$

The resulting island is created on a resonant surface with $q = m/n$ and its half-width $\delta_{m,n}$ is given by the formula [11]

$$\delta_{m,n} = \sqrt{\frac{8q^2\tilde{b}^1_{(m,n)}}{q'm}} \tag{2}$$

where $q' \equiv dq/ds$.

To quantify the overlap of magnetic islands on neighboring rational surfaces with the same value of n we use the Chirikov parameter σ_{Chir} defined as $\sigma_{\text{Chir}} \equiv (\delta_{m,n} + \delta_{m,n})/\Delta_{m,n}$ where $\delta_{m,n}$ is defined in (2) and $\Delta_{m,n}$ is the radial distance (in terms of the coordinate s) between the surfaces

with $q = m/n$ and $q = (m+1)/n$. The criterion for island overlap is $\sigma_{\text{Chir}} > 1$. (However, transition to stochasticity occurs for smaller values of σ_{Chir} because of secondary island chains which appear between the primary ones. Islands created by perturbation modes with another toroidal number n will also facilitate the transition to stochasticity by "filling in gaps" between the islands with one value of n.) The transition to stochasticity can be verified by tracing the field lines and displaying the Poincaré plot of their intersections with a chosen poloidal plane. Such plot will clearly show the magnetic islands, the stochastic areas and remaining magnetic surfaces between them.

For actual calculations we used the code ERGOS [8], which had been previously used for the cases of DIII-D [9], JET, MAST [7] and proposed designs of the ITER RMP coils [8], for example. The input to the code is the configuration of the coils (given by their geometry and current distributions) and the magnetic equilibrium. The equilibrium is needed for calculating the contravariant component B^1, for transforming to the magnetic coordinate system (s, θ^*, φ), and for knowing the profile of q and its derivative q', which are in turn needed to know the positions and sizes of the magnetic islands – Eq. (2). The perturbation spectra thus depend on the equilibrium.

The output of the code is the profile of σ_{Chir}, radial dependence of the perturbation spectrum (dependence of $\tilde{b}^1_{(m,n)}$ on s) and the Poincaré plot resulting from field line tracing in the perturbed magnetic field.

3. Techniques for spectrum optimization

Especially in the case of a new coil design or of choosing a configuration of a very flexible coil system (as it is the case of COMPASS) it is useful to have general rules which allow to heuristically choose a good configuration. For the application we are interested in an optimal configuration maximizes the overlap of islands at the plasma edge for a given coil current (governed by technical and financial constraints).

As the island sizes are given by the value of $\tilde{b}^1_{(m,n)}$ at the radial position s where $q(s) = m/n$, they will be maximized when the maxima of $\tilde{b}^1_{(m,n)}(s)$ in the (m,s) space are located at the points where the condition $q(s) = m/n$ holds. This can be checked graphically by plotting $\tilde{b}^1_{(m,n)}(s)$ as a function of (m,s) and checking the overlap of its maxima with the safety factor profile given by $q(s) = m/n$. This gives an indication if the maximal value of $\tilde{b}^1_{(m,n)}(s)$ needs to be moved to higher or lower values of m, which can be done by making the coils narrower or larger, respectively. (In this procedure n is kept constant, it is assumed that there is one dominant toroidal mode, corresponding to the toroidal symmetry of the coils.)

The resonances at the edge, where the q is high, occur for large values of m. To obtain a $\tilde{b}^1_{(m,n)}$ spectrum with a maximum at high values of m the corresponding b^1 as a function of θ^* must be narrow in the θ^* space. To achieve this it is preferable to place the coils at the low-field side (LFS) where θ^* changes slowly as a function of the geometric poloidal angle, corresponding to the steep pitch angle of the field lines at this place. (This is caused by the toroidal geometry.) Moreover the Shafranov shift of magnetic surfaces outwards causes ∇s to be maximal at the LFS which maximizes the value of b^1, being given by the contravariant radial component: $b^1 = B^1/B^3 = (\delta \vec{B} \cdot \nabla s)/(\vec{B} \cdot \nabla \varphi)$. At the same time the denominator B^3 is minimized because of the low toroidal magnetic field. All those geometric effects make the LFS the optimal place for placing the perturbation coils [11].

To estimate what are the best coil positions for a given equilibrium it is useful to display possible coil positions in a poloidal cross-section together with the mesh of (s, θ^*) magnetic coordinates.

The coils produce radial perturbation which is directed either inwards or outwards. If the coils are symmetric with respect to the midplane, there may be an "even" configuration (where an upper coil has the same field orientation as the symmetric lower coil) or an "odd" one (where upper and lower coils have opposite fields). For an even configuration the maxima and minima of the radial perturbation shall correspond to maxima and minima of the function $\cos(m\theta^*)$ on a resonant surface with $q(s) = m/n$ to maximize the Fourier component $\tilde{b}^1_{(m,n)}(s)$ on that surface. For an odd configuration the perturbation should correspond to $\sin(m\theta^*)$. (The coordinate θ^* is chosen to be zero at the outboard midplane, so $\cos(m\theta^*)$ and $\sin(m\theta^*)$ are even and odd functions respectively with respect to the midplane.) To do that we display the sign of $\cos(m\theta^*)$ or $\sin(m\theta^*)$ on resonant surfaces and place the coil loops so that one direction of the field is close to areas with positive sign and other direction to areas of negative sign. The toroidal coil segments which separate the coil loops shall be placed against zeros of $\sin(m\theta^*)$ or $\cos(m\theta^*)$.

4. COMPASS RMP coils

Each of the four quadrants of the vacuum vessel of COMPASS is covered by a set of toroidal and poloidal coil segments[1] to produce resonant magnetic perturbations (RMPs). Because of the four-fold symmetry the main toroidal mode number n can be 1 or 2. The symmetry is only approximate however, the poloidal positions of the outer toroidal segments are different in each quadrant and there are many irregularities as the coils need to avoid the ports. The toroidal segments at the outboard midplane are also missing from two quadrants because of large midplane ports. This means that a configuration avoiding those segments will have better toroidal symmetry and a dominant $n = 2$ toroidal mode. All the coil segments can be connected independently. In principle there is enormous number of possibilities for the configurations distinguished by the current directions in the segments. In addition the four outer toroidal segments in each quadrant can be moved in the poloidal direction, which adds another degrees of freedom in the configuration. But only a small percentage of the configurations are practical. We are looking for configurations that are mostly toroidally symmetric (we focus on $n = 2$ toroidal mode) and use the outermost coils for the reasons given in Section 3. Moreover there is a constraint that at every point where several coils meet the sum of incoming and outgoing currents from the power supplies should be zero. The bars which connect the coils to the linkboards are for all such points close to each other so if the total current in such a bundle of bars is zero, the total force from the toroidal field will be also zero, minimizing the mechanical stress [12]. It is also ensured that the bars will not create stray fields, thus we don't need to include them in the coil model. This constraint means that the coils can be effectively thought of as a sum of closed loops, with some segments shared between two loops (their current will be two times higher compared to the others).
All the above-mentioned requirements determine what coils should be used and the directions of their currents. The positions of the movable coil segments shall be tuned to the magnetic equilibrium using the methods described in Section 3.

5. Results for selected equilibria

To demonstrate the ability of producing overlapping islands at the edge we used several equilibria that we believe to be representative for the future operation of COMPASS. Those equilibria

---

[1]They are sometimes called "saddle coils", not to be confused with "saddle loops" which are diagnostic coils to measure the radial magnetic flux.
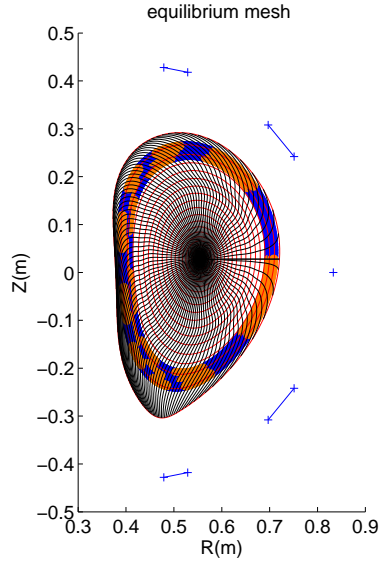
FIG. 1. *Magnetic coordinates for the SNT-02 case, with* $\mathrm{sgn}\sin(m\theta^*)$ *shown as blue (positive) and orange (negative) dots. Possible positions of movable coils are shown as blue lines.*
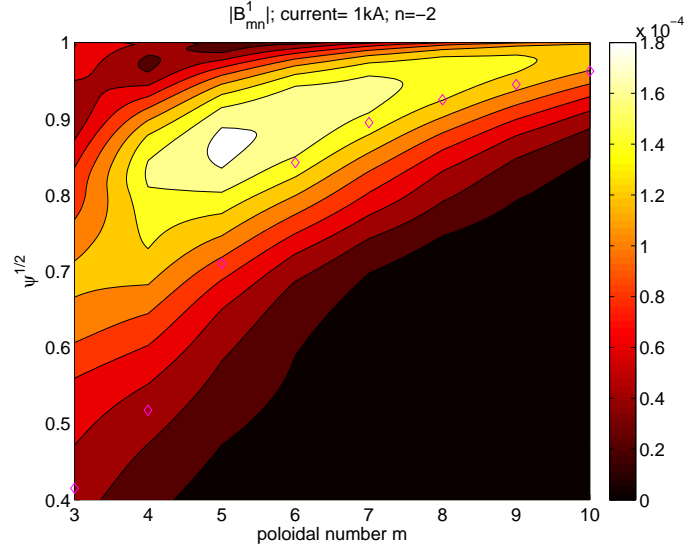
FIG. 2. *Spectrum of* $\tilde{b}^1_{(m,n)}$ *and the q profile (diamonds) for the SNT-02 case.*

are predicted by the MHD code ACCOME [13], taking into account the planned neutral beam injection and lower hybrid current drive, which together produce a substantial fraction of the current [14]. The equilibria are:

- SNT-02 – a high field, high current (B=2.1 T, I=250 kA) equilibrium with a high triangularity ($\delta = 0.5 - 0.7$)

- SND-02 – a high field, high current equilibrium with a low triangularity ($\delta = 0.3 - 0.4$)

- SND-01 – a low field, low current (B=1.2 T, I=175 kA) equilibrium with a low triangularity ($\delta = 0.3 - 0.4$).

The code HELENA [15] is used to produce the mapping to the magnetic coordinate system used by ERGOS.

FIG. 1 shows the magnetic coordinate system of the SNT-02 equilibrium. An odd parity configuration needs to be used. Sign of $\sin(m\theta^*)$ is shown in color for several resonant surfaces. Also shown are the ranges of positions of the outer movable toroidal coil segments. It can be seen that to match the equilibrium the outermost possible positions shall be used. They still don't match the positions of zeros of $\sin(m\theta^*)$ precisely. It can be also seen that at the LFS the zeros of $\sin(m\theta^*)$ are well aligned between different magnetic surfaces. This means that we can optimize the spectrum at a range of surfaces simultaneously, which is advantageous to obtain a good overlap of islands. The radial dependence of spectrum shown in FIG. 2 confirms these conclusions. The maxima of the spectra occur at smaller values of m that correspond to the q profile, which means that it would be beneficial to move the coils even more outwards to produce a narrower perturbation, if there were such a possibility. The maxima of the spectrum form a curve in the (m,s) space which is parallel to the q profile, so the same conclusion holds for all radial positions at the edge. (This confirms the conclusion about simultaneous optimizing for a range of radial positions and is a fairly generic feature of the edge perturbation spectra.)
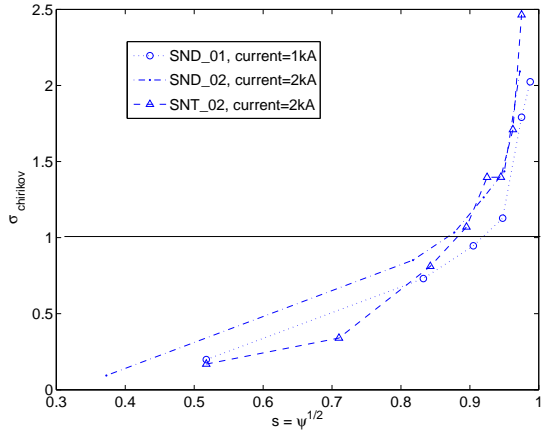
FIG. 3. *Radial dependence of the Chirikov parameter for the equilibria considered.*
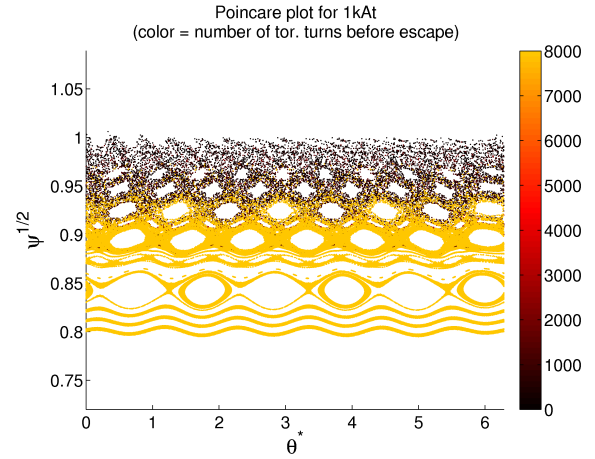

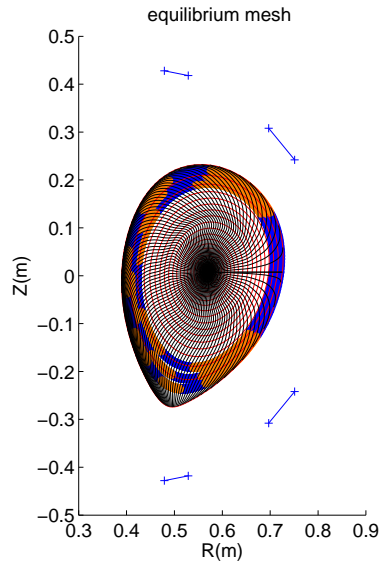FIG. 4. *Poincaré plot for the SNT-02 case, coil current 1 kA.*

FIG. 5. *Magnetic coordinates for the SND-01 case, with* $\mathrm{sgn}\cos(m\theta^*)$ *and coil positions shown as in FIG. 1.*

FIG. 3 shows the resulting profile of the Chirikov parameter. We have shown that the available coil positions are not ideal, but despite this there is a good island overlap in the edge region for a current in the coils of 2 kA. (Some coil segments will have twice as much current, i.e. 4 kA. The coils are designed for a maximum current of 5 kA.). FIG. 4 shows the resulting Poincaré plot for a current of 1 kA. Even for this smaller value of current a stochastic region appears because of the secondary island chains that facilitate the transition to stochasticity.

The SND-02 equilibrium has similar properties as the SNT-02 one with respect to the conclusions about optimal placing of the coils and the resulting spectrum, which is thus not shown for brevity. This is related to a similar value of q_{95} between these two. The profile of the Chirikov parameter is shown in FIG. 3.

The SND-01 equilibrium has a substantially lower q_{95} than the preceding two. Zeros of $\sin(m\theta^*)$ are much more distant poloidally which could be accommodated for by moving the coils outwards to produce a wider perturbation. It is more practical however to use an even parity configuration which keeps the coils at the same place but uses a large loop in the midplane
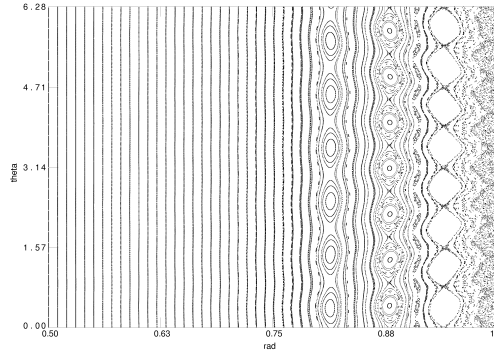
FIG. 6. Poincaré plot of the magnetic field resulting from RMHD modelling.

for a perturbation wider in the poloidal direction. The reason is technical: while the coils are movable in principle, it is preferable to avoid readjusting them between shots because of access difficulties. It will be much easier to rewire the coils for different currents, as this is done on linkboards designed for easy reconfiguration. By avoiding the midplane coil segments we also obtain better symmetry and a stronger main $n = 2$ toroidal component. Because of the even parity the positions of the coils should be compared against zeros of $\cos(m\theta^*)$. Sign of $\cos(m\theta^*)$ on several resonant surfaces is shown together with the coordinate mesh on FIG. 5. Again the coil positions are not ideally matched to the equilibrium, but the resulting island overlap (FIG. 3) is very good even at a current of 1 kA.

6. Reduced MHD simulations of field penetration

The vacuum approximation described above does not take into account modification of the perturbation field by the plasma response. The perturbation field interacting with the plasma rotation produces helical current, which in turn reduce the perturbation. To estimate this effect we have performed reduced MHD simulations with the cylindrical code described in [16] and [17]. The vacuum harmonics of the perturbed magnetic potential ψ from the ERGOS calculations are used as boundary conditions for the reduced MHD code. This code treats plasma as a straight cylinder with a circular cross-section to be able to work with toroidal and poloidal Fourier harmonics of the plasma variables, which results in significant speed, memory usage and simplicity gains. Unfortunately the large values of q near the edge resulting from the X-point geometry can not be treated unless an unphysical negative current density were introduced.

The simulations were done for the SNT-02 case, current of 1 kA and several values of toroidal velocity. FIG. 6 shows the resulting Poincaré for toroidal rotation frequency of 12 kHz. We can see that edge islands remain, while the $m = 6$ one located more towards the center is reduced in size. The stochastic region is reduced, however that is the consequence of the much reduced magnetic shear due to the cylindrical geometry, which makes islands more separated and prevents island overlap.

7. Conclusions

We have demonstrated that for a wide variety of magnetic equilibria the perturbation coils on the COMPASS tokamak are able to produce overlapping magnetic islands at the plasma edge. We are thus confident in the relevance of planned experiments with the magnetic perturbations to the research of interactions of resonant magnetic perturbations with plasma, especially the mechanism of ELM suppression. We developed methods for optimizing the coil geometry and

we have used them to specify the required positions of the perturbation coils. The result will be used to configure the coils before COMPASS operation starts. It is encouraging that so far we have not found necessary to adjust the coil positions differently for different plasma parameters, which will facilitate the operation a lot.

The reduced MHD simulations have shown that the islands in the edge region remain when the plasma response is taken into account. The simulations should be considered very preliminary and should be repeated when more precise plasma parameters are known either from modelling or from first experiments. For example the knowledge of the H-mode pedestal will enable us to include diamagnetic effects due to strong pressure gradients, which have not been included so far.

References

[1] Evans, T., et al., Nucl. Fusion **48** (2008), 024002.

[2] Liang, Y., et al., Phys. Rev. Lett. **98** (2007), 265004.

[3] Panek, R., et al., Czech. J. Phys. **56** (2006), B125.

[4] Fitzpatrick, R., Physics of Plasmas **5** (1998), 3325.

[5] Shaing, K.C., Physics of Plasmas **10** (2003), 1443.

[6] Fenstermacher, M.E., et al., Phys. Plasmas **15** (2008), 056122.

[7] Nardon, E., et al., "ELM control by resonant magnetic perturbations on JET and MAST," Submitted to J. Nucl. Mater.

[8] Bécoulet, M., et al., Nucl. Fusion **48** (2008), 024003.

[9] Bécoulet, M., et al., Nucl. Fusion **45** (2005), 1284.

[10] Nardon, E., et al., J. Nucl. Mater. **363-365** (2007), 1071.

[11] Nardon, E., Edge localized modes control by resonant magnetic perturbations, Ph.D. thesis, Ecole Polytechnique (2007).

[12] Todd, T., personal communication (2008).

[13] Tani, K., et al., Journal of Computational Physics **98** (1992), 332.

[14] Fuchs, V., et al., in "Proceedings of the 35th EPS Conference on Plasma Physics," , vol. 32F of *Europhysics Conference Abstracts* (2008), pp. P–2.098.

[15] Huysmans, G., et al., in "Proc. CP90 Europhysics Conf. on Comput. Phys.", (1991), p. 371.

[16] Bécoulet, M., et al., paper TH/2-1Ra, these Proceedings (2008).

[17] Nardon, E., et al., Phys. Plasmas **14** (2007), 092501.